Chemical Engineering Communications, 203:516–526, 2016

ISSN: 0098-6445 print/1563-5201 online
DOI: 10.1080/00986445.2015.1048799

Taylor & Francis
Taylor & Francis Group

Identification and Online Validation of a pH Neutralization Process Using an Adaptive Network-Based Fuzzy Inference System

ARIANE SILVA MOTA[1], MAURO RENAULT MENEZES[1], JONES ERNI SCHMITZ[2], THIAGO VAZ DA COSTA[3], FLÁVIO VASCONCELOS DA SILVA[4], and IVAN CARLOS FRANCO[1,4]

[1]*Department of Chemical Engineering, University Center of FEI, São Bernardo do Campo, SP, Brazil*
[2]*Department of Exact and Earth Science, Federal University of São Paulo-UNIFESP, Diadema, SP, Brazil*
[3]*School of Chemical Engineering, Federal University of Itajubá-UNIFEI, Itajubá, MG, Brazil*
[4]*School of Chemical Engineering, University of Campinas-UNICAMP, Campinas, SP, Brazil*

In this study, the application of adaptive neuro-fuzzy inference system (ANFIS) architecture to build prediction models that represent the pH neutralization process is proposed. The dataset used to identify the process was obtained experimentally in a bench scale plant. The prediction model attained was validated offline and online and demonstrated as able to precisely predict the one step-ahead value of effluent pH leaving the neutralization reactor. The input variables were the current and one past value of the acid and base flow rates and the current value of the output variable. Variance accounted for (VAF) indices greater than 99% were achieved by the model in experiments in which the disturbances in the acid and basic solutions flow rates were applied separately. For tests with simultaneous disturbances, conditions never seen in the training and suffering from reactor level oscillations, the prediction model VAF index was still approximately 96%. The validations demonstrated the capability of ANFIS to build precise fuzzy models from input–output datasets. R^2 values achieved were always larger than 0.96.

Keywords: ANFIS architecture; pH neutralization; prediction models; process identification

Introduction

pH is an important variable in many branches of industry. For example, it affects the growth of microbes in bioprocesses and influences the efficiency of catalysts used in chemical reactions and the characteristics of the materials that make up the industrial equipment. Also, it affects human and animal health. Thus, products like food, medicines, and cosmetics should be developed considering harmless pH ranges. Therefore, rigorous control of pH is needed to improve reaction yield and product quality and to comply with environmental and safety requirements. However, the dynamics of pH processes exhibit nonlinear time-varying characteristics (Henson and Seborg, 1994; Kumbasar et al., 2011). As a consequence, conventional linear controllers are unable to adequately regulate these processes and advanced control strategies are required. In this context, process identification is a fundamental task. Besides, process models could be also used for other purposes like equipment design, operator training, and fault detection.

Artificial intelligence techniques have been valuable tools for system identification for a long time (Bath and McAvoy, 1990; Gustafsson et al., 1995; Draeger et al., 1995; Palancar et al., 1998). Bath and McAvoy (1990) proposed the application of artificial neural networks (ANNs) for chemical process modeling. ANNs were also used by Gustafsson et al. (1995) in a pH control strategy and by Palancar et al. (1998) to predict future pH values and as an inverse model in a pH control system. In a similar way, inverse fuzzy models were embedded in a control system by Kumbasar et al. (2011). Mwembeshi et al. (2004) investigated the algorithms employed in the learning of neural networks used to represent the process gain characteristics of pH reactors. Valarmathi et al. (2009) applied ANNs and genetic algorithms for the identification and control of a pH process.

Identification strategies that take advantage of the reasoning capacity of fuzzy inference systems (FIS) coupled with the learning and function approximation capabilities of neural networks have been suggested. A fuzzy-neural approach was proposed by Nie et al. (1996) to model a pH neutralization process. In this approach, self-organizing schemes were used to construct the rule base required by fuzzy reasoning models. In the recurrent neuro-fuzzy

Address correspondence to Ivan Carlos Franco, Department of Chemical Engineering, University Center of FEI, Av. Humberto Alencar Castelo Branco, 3972, CEP: 09850-901, São Bernardo do Campo-SP, Brazil. E-mail: icfranco@fei.edu.br

Color versions of one or more of the figures in the article can be found online at www.tandfonline.com/gcec.

network proposed by Zhang and Morris (1999), expert knowledge is used to divide the operating region into several fuzzy models; these local models are adjusted to fit the input–output data. The resulting network is able to provide long-term predictions required by a predictive controller.

Adaptive neuro-fuzzy inference system (ANFIS) has been successfully applied for the identification of complex systems. The ANFIS architecture was described by Jang (1993); it combines the semantic transparency of fuzzy rule-based systems with the learning capability of neural networks. The result is an approach which can learn an input–output behavior from a dataset and tune the fuzzy rule base, reducing the influence of the human expert required by FIS. Chang and Chang (2006) applied ANFIS to build a prediction model for water reservoir management. The reservoir level behavior presents nonlinearities, uncertainty, and time-varying characteristics. The authors concluded that ANFIS models are useful for predicting the reservoir level, becoming a valuable tool for flood control operations. Franco et al. (2011) applied an identification technique based on ANFIS architecture for the prediction of the temperatures of a chiller system. Chiller systems are used to cool liquids and present nonlinear and interacting behavior. The results attained by the models showed good agreement with experimental data, in both offline and online validation. Recently, Jahedsaravani et al. (2014) applied both ANFIS and a nonlinear regression technique to model a froth flotation process. By comparing the results, the former approach demonstrated to be more efficient than the statistical approach for this complex process. Another application of the ANFIS model was accomplished by Fernandez de Cañete et al. (2013). In this case, the authors described an ANFIS scheme for the control of a distillation column. A study presented by Abonyi et al. (1999) described the use of a learning algorithm based on a gradient descent adaptive fuzzy controller. The proposed approach was applied to a fuzzy control structure based on an inverse model for a nonlinear plant. Postlethwaite and Edgard (2000) developed an algorithm for a MIMO (Multiple-Input-Multiple-Output) controller that calculates, from a MIMO fuzzy model, the control actions at each sampling interval. The control was tested in simulations of pH control.

The aim of this study is to develop the methodology to achieve accurate models of a pH neutralization process using the ANFIS architecture. In the following section, a description of the ANFIS architecture is presented. In the section "Material and Methods," the pH neutralization plant and the experimental methodology are described. Then, the results of the experiments are discussed and conclusions drawn.

Identification Using ANFIS Architecture

The major aim of works combining FIS and ANNs is to use ANNs to systematize the adjustment of the FIS membership function parameters. Therefore, the FIS ability to deal with nonlinear, incomplete, and imprecise data can be exploited for identification and control purposes.

ANFIS combines the back-propagation gradient descent method and the least-squares method to update the FIS membership function parameters in an adaptive network. A schematic representation of the ANFIS architecture proposed is shown in Figure 1.

The structure of the FIS could be determined using the subtractive clustering method (Paiva and Dourado, 2004). Subtractive clustering is an efficient method that is used

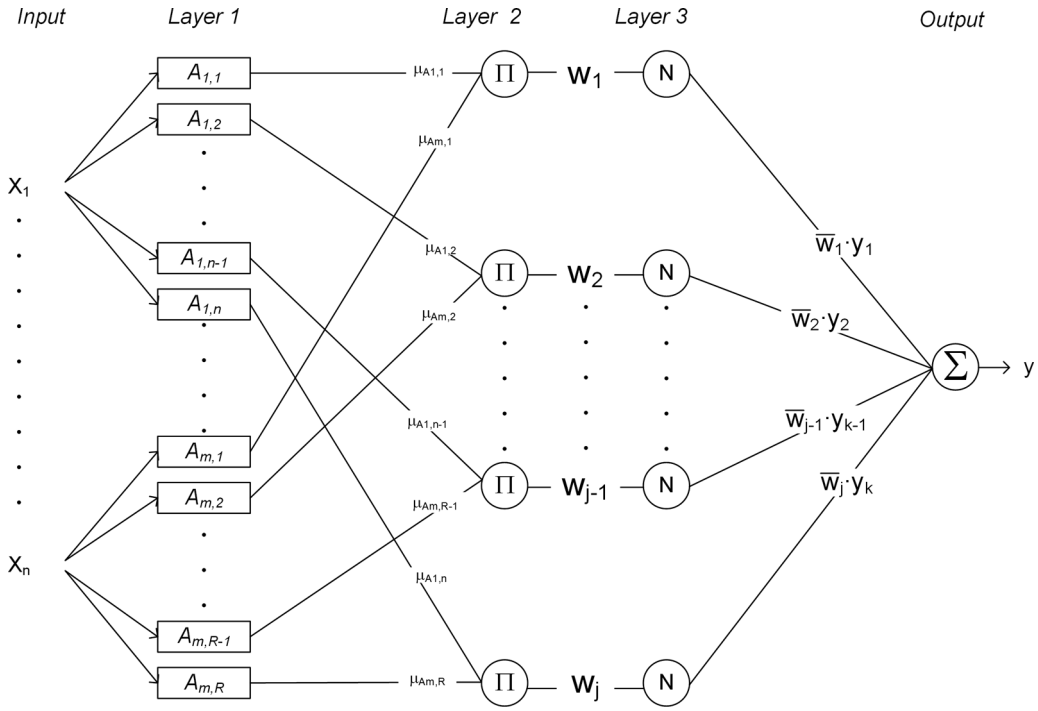

Fig. 1. Schematic representation of the ANFIS architecture.

without *a priori* information of the number of clusters. It avoids any use of optimization algorithms and could provide the number of clusters and their centers (Chiu, 1994).

The network training is carried out using a dataset and is based on the back-propagation method. Therefore, the network parameters are initialized, the input signal is propagated by the subsequent layers, and the output is calculated. This calculated output is compared with the original output. Then, the error signal is propagated backward and the parameters are updated. The output of each layer is calculated as:

$$\text{Layer 1} : \mu_{Ak,j}(x_k) = \mathrm{e}^{-\frac{(x_k - c_j)^2}{2\sigma_j^2}} \tag{1}$$

where $\mu_{Ak,j}$ are the membership functions for the linguistic labels Ak,j; x_k is the k-th input; j represents the linguistic variables; c_j is the cluster center; and σ_j is the dispersion of the cluster.

$$\text{Layer 2} : w_j = \prod_{k=1}^{n} \mu_{Ak,j}(x_k) \tag{2}$$

where n is the number of inputs.

$$\text{Layer 3} : \bar{w}_j = \frac{w_j}{\sum_{r=1}^{n} w_r} \tag{3}$$

And,

$$\bar{w}_j y_j = \bar{w}_j (q_{j0} + q_{ji} x_i + \ldots + q_{jn} x_n) \tag{4}$$

where q_{ji} are the consequent parameters.

$$\text{Output} : y = \sum_{j=1}^{N} \bar{w}_j y_j \tag{5}$$

where N is the number of linguistic variables.

The premise parameters (c and σ) are updated using the gradient descent method, while the consequent parameters (q) are calculated by means of least-squares method. More details are presented in Jang (1993).

Material and Methods

Experimental Facilities

The pH neutralization bench scale plant used in the experiments is shown in Figure 2. In Figure 3, the instrumentation diagram is illustrated. The apparatus consisted of a continuous stirred-tank reactor (CSTR), two peristaltic pumps used to feed acid and basic solutions into the reactor, two feed tanks to retain the solutions before entering the reactor, two reservoirs of the acid and basic solutions, the level sensor (magnetic), the pH sensor, four data converters, and the frequency inverter. There were also two peristaltic pumps used to transfer acid and basic solutions from the reservoirs to the feed tanks and another used to dispose of the effluent. The data communication system was based on the Fieldbus protocol.

In all of the experiments, the level of liquid inside the reactor was controlled to remain at 30%.

Fig. 2. Experimental facilities picture: 1: fieldbus communication module; 2: frequency inverter; 3: fieldbus converter; 4: pH converter; 5: computer; 6: level sensor; 7: pH sensor; 8: reactor; 9: pump (acid); 10: pump (basic); 11: pump (effluent); 12: feed tanks; 13: reservoirs.

Process Identification and Validation

Experiments were carried out to obtain experimental data required to identify and validate the pH neutralization process. Each of these experiments consisted of three steps: determination of process settling time; ANFIS training and offline validation; and online validation. In all of the experiments, solutions of NaOH and HCl with equal concentrations of $4 \times 10^{-3}\,\mathrm{mol \cdot L^{-1}}$ were used.

Determination of Settling Time

The settling times of the process (t_s) were obtained by initially keeping both acid and basic solution flow rates constant; after the outlet effluent pH reached steady-state conditions, step changes were applied to one of the flow rates. In the first run (R1a), the acid solution flow rate (Q_{HCl}) was kept constant at $15.0\,\mathrm{L \cdot h^{-1}}$ and step changes were introduced in the flow rate of the basic solution (Q_{NaOH}), as presented in the first column of Table I. Another run (R1b) was performed keeping the basic solution flow rate constant at $9.0\,\mathrm{L \cdot h^{-1}}$ and changing the acid solution flow rate as indicated in the second column of Table I. Analyzing the pH of the effluent leaving the reactor, it was possible to determine the settling times. These settling times enabled the calculation of the switching times. Switching time is used to

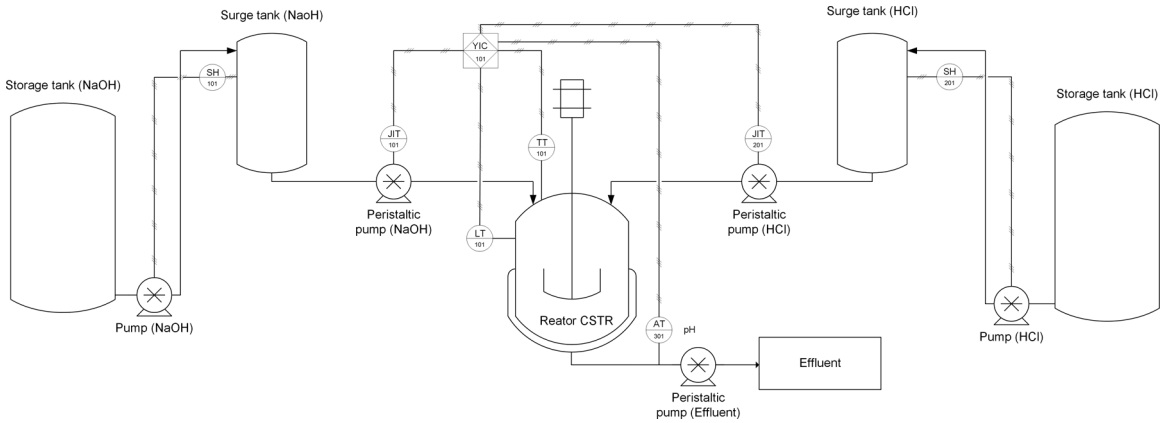

Fig. 3. Instrumentation flowchart of the pH neutralization pilot plant.

design input signals that preserve the details of process dynamics; it is the minimum time between changes in each input variable. It could be calculated using Equation (6) (Seborg et al., 2004):

$$t_{sw} = \frac{t_s}{3} \tag{6}$$

ANFIS Training and Offline Validation

An experiment was carried out introducing random changes in both Q_{HCl} and Q_{NaOH}; these changes are introduced in accordance with the switch times. The data obtained were used to train ANFIS and to validate the Takagi–Sugeno models used in the prediction of the outlet effluent pH. The Fuzzy Logic Toolbox of Mathworks was used to train and build the models.

Online Validation

The prediction models were tested online. In this experiment, random changes were applied to the process and outlet effluent pH responses were compared with predicted values in real time.

Results and Discussion

Switching Times

The experiments R1a and R1b were performed, and the results are shown in Figures 4 and 5, respectively. The outlet effluent pH response to each change in Q_{HCl} or Q_{NaOH} was analyzed using these figures. The settling times achieved are presented in Table II.

Table I. Changes applied in Q_{NaOH} and in Q_{HCl} in runs R1a and R1b, respectively

Changes in Q_{NaOH} ($L \cdot h^{-1}$)	Changes in Q_{HCl} ($L \cdot h^{-1}$)
13.0–20.0	9.0–12.0
13.0–25.0	9.0–12.0
13.0–30.0	9.0–12.0
13.0–10.0	9.0–6.0
13.0–5.0	9.0–3.0
13.0–0	

The greatest value of settling time was used to calculate the respective switch time. So, the switch times relative to changes in Q_{NaOH} and Q_{HCl} are 133.0 s and 167.0 s, respectively.

Training and Offline Validation

The reactor outlet effluent pH response to the disturbances in acid and basic solutions flow rates are shown in Figure 6. These disturbances were applied according to the switch times of each variable.

Data presented in Figure 6 were used to build the Takagi–Sugeno prediction models employing an ANFIS architecture and to validate such models. Before the ANFIS training, data presented in Figure 6 were discretized using a sampling time of 10 s and transformed into deviation variables. A deviation variable, $\bar{y}(k)$, is the difference between the current value of the variable, $y(k)$, and its value in the steady state. Here, the first 70% of the data were used in the identification and

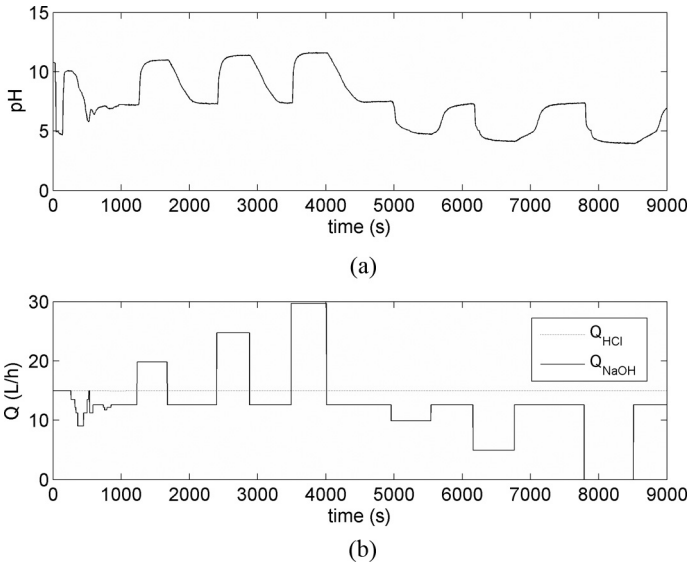

Fig. 4. Experiment R1a: (a) outlet effluent pH response and (b) Q_{HCl} and Q_{NaOH} flow rates.

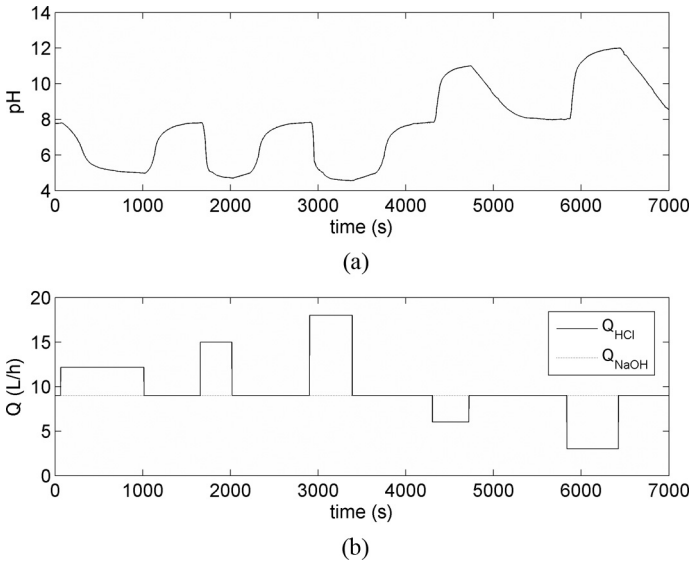

Fig. 5. Experiment R1b: (a) outlet effluent pH response and (b) Q_{HCl} and Q_{NaOH} flow rates.

Table II. Settling times from experiments R1a and R1b

Settling times for experiment R1a (s)	Settling times for experiment R1b (s)
260.0	350.0
280.0	280.0
230.0	296.0
400.0	370.0
400.0	500.0
400.0	

the remaining 30% were used in the offline validation of the models. Each input vector was composed by $\bar{Q}_{NaOH}(k-2)$, $\bar{Q}_{NaOH}(k-1)$, $\bar{Q}_{HCl}(k-2)$, $\bar{Q}_{HCl}(k-1)$, and $\overline{pH}(k-1)$. The output was the one step-ahead value of the reactor outlet effluent pH, $\overline{pH}(k)$. Values used in the training are illustrated in Figure 7.

Gaussian membership functions were chosen for the inputs. Before the training, the subtractive clustering technique was applied to establish the better number of rules. This better configuration of membership functions is shown in Figure 8. Linguistic variables representing the antecedents were: "VL" for very low, "L" for low, "M" for medium, "H" for high, and "VH" for very high. The training and successive subtractive clustering resulting rules are presented in Table III.

The linear functions that represent the output variable, pH_i for $i=1,\ldots,5$, in each fuzzy rule were obtained as follows:

$$\begin{aligned} pH_i = {} & q_0 + q_1\bar{Q}_{NaOH}(k-1) + q_2\bar{Q}_{NaOH}(k-2) \\ & + q_3\bar{Q}_{HCl}(k-1) + q_4\bar{Q}_{HCl}(k-2) \\ & + q_5\overline{pH}(k-1),\ i=1,\ldots,5 \end{aligned} \tag{7}$$

The consequent parameters are presented in Table IV.

The validation was performed using a model characterized by rules presented in Tables IV and V and the membership functions illustrated in Figure 8. A comparison of the predicted values with the real values is shown in Figure 9.

From Figure 9, is possible to verify that the model was able to adequately predict the one step-ahead value of the reactor outlet effluent pH. The analysis of data dispersion supports this conclusion (Figure 10).

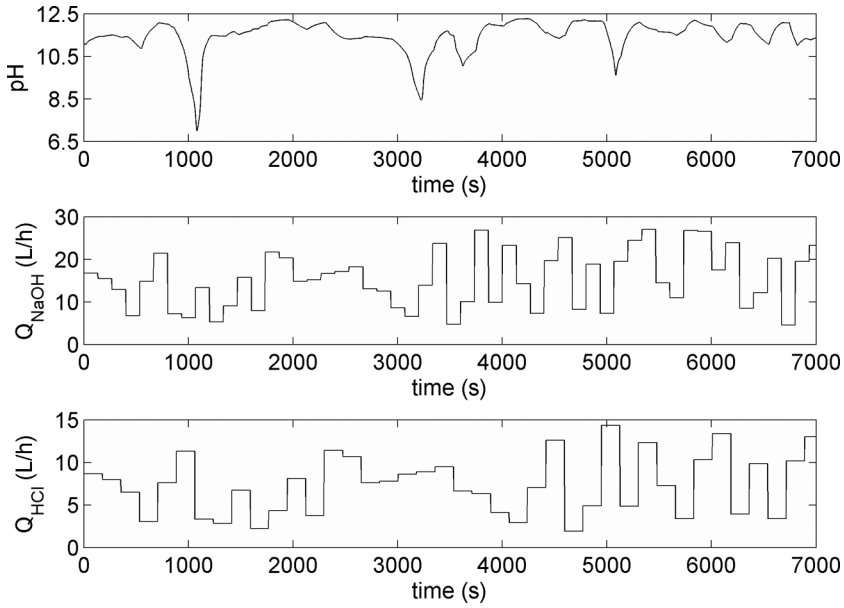

Fig. 6. Reactor outlet effluent pH response to disturbances in Q_{NaOH} and Q_{HCl}.

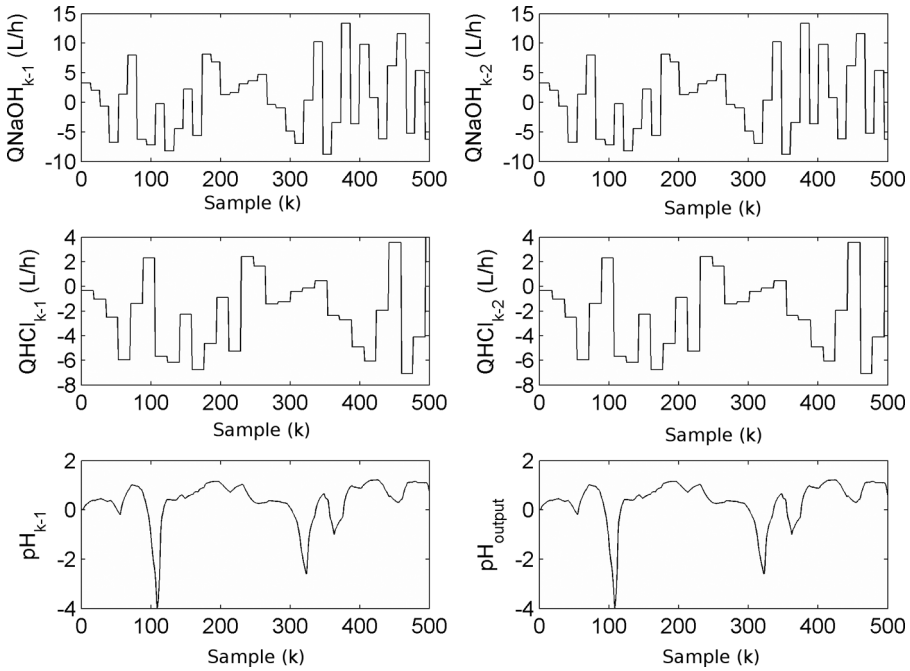

Fig. 7. Data used to train the ANFIS.

Online Validation

The online validation of the prediction model was carried out in two different conditions. In the first run (V1), simultaneous random disturbances in Q_{NaOH} and Q_{HCl} were applied. In the second run (V2), the values of Q_{NaOH} and Q_{HCl} were shifted individually. The range of input and output data used in training and in validation steps are presented in Table V.

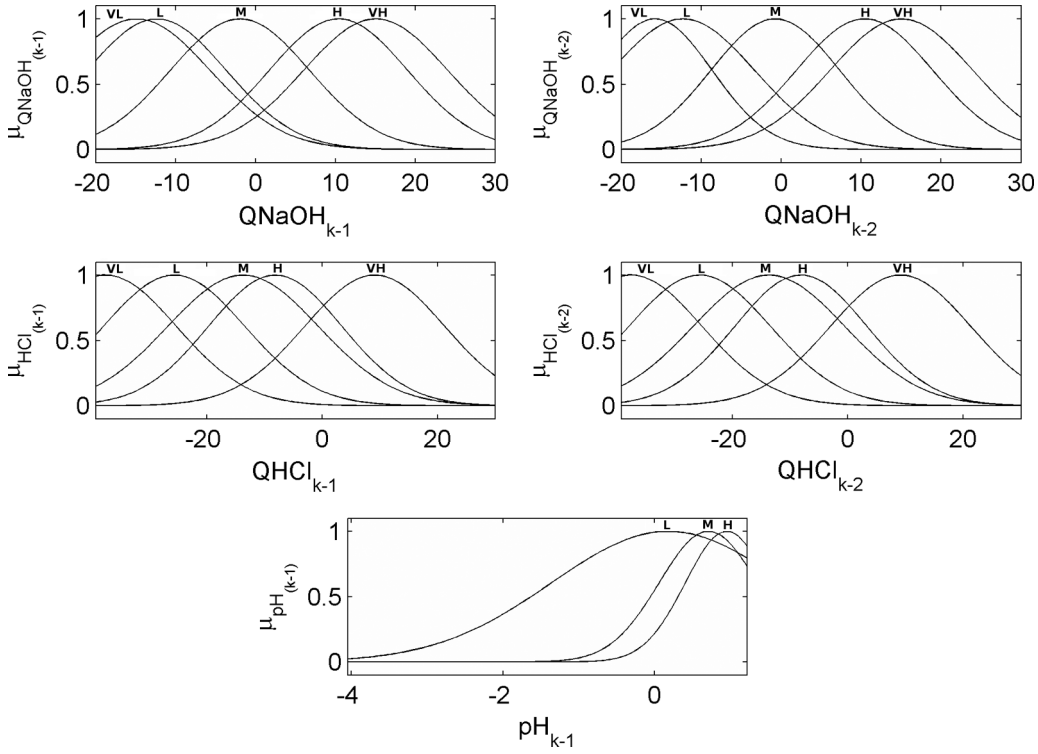

Fig. 8. Fuzzy sets and membership functions of the Takagi–Sugeno prediction model.

Table III. Fuzzy rules of the Takagi–Sugeno prediction model

	Fuzzy rule
1	If $\bar{Q}_{NaOH}(k-1)$ is M and $\bar{Q}_{NaOH}(k-2)$ is M and $\bar{Q}_{HCl}(k-1)$ is H and $\bar{Q}_{HCl}(k-2)$ is H then $\overline{pH}(k)$ is pH_1.
2	If $\bar{Q}_{NaOH}(k-1)$ is VH and $\bar{Q}_{NaOH}(k-2)$ is VH and $\bar{Q}_{HCl}(k-1)$ is L and $\bar{Q}_{HCl}(k-2)$ is L and $\overline{pH}(k-1)$ is M then $\overline{pH}(k)$ is pH_2.
3	If $\bar{Q}_{NaOH}(k-1)$ is L and $\bar{Q}_{NaOH}(k-2)$ is L and $\bar{Q}_{HCl}(k-1)$ is VL and $\bar{Q}_{HCl}(k-2)$ is VL and $\overline{pH}(k-1)$ is VH then $\overline{pH}(k)$ is pH_3.
4	If $\bar{Q}_{NaOH}(k-1)$ is H and $\bar{Q}_{NaOH}(k-2)$ is H and $\bar{Q}_{HCl}(k-1)$ is VH and $\bar{Q}_{HCl}(k-2)$ is VH and $\overline{pH}(k-1)$ is VL then $\overline{pH}(k)$ is pH_4.
5	If $\bar{Q}_{NaOH}(k-1)$ is VL and $\bar{Q}_{NaOH}(k-2)$ is VL and $\bar{Q}_{HCl}(k-1)$ is M and $\bar{Q}_{HCl}(k-2)$ is M then $\overline{pH}(k)$ is pH_5.

Table V. Ranges of input and output variables values

	Training	Offline validation	Online validation, V1	Online validation, V2
pH				
Minimum	7.0	9.2	11.4	8.4
Maximum	12.3	12.2	12.1	12.0
Q_{NaOH} ($L \cdot h^{-1}$)				
Minimum	4.7	4.5	5.3	9.0
Maximum	26.8	27.0	21.7	18.0
Q_{HCl} ($L \cdot h^{-1}$)				
Minimum	1.9	3.3	2.2	7.2
Maximum	14.3	14.4	11.4	10.8

Results of V1

The behavior of reactor outlet effluent pH in front of simultaneous changes in Q_{NaOH} and Q_{HCl} and the predicted values are illustrated in Figure 11(a); the disturbances applied in Q_{NaOH} and Q_{HCl} are presented in Figures 11(b) and 11(c), respectively.

The predicted values present excellent agreement with experimental values for almost all of the experiments. The results of the dispersion analysis are presented in Figure 12.

However, in two situations, when the values of Q_{NaOH} and Q_{HCl} were approximately $13\,L \cdot h^{-1}$ and $6.5\,L \cdot h^{-1}$, respectively (with intervals of 300–500 s and 1300–1500s, respectively), the predicted and real trends were detached. This can be justified as a consequence of the lack of similar conditions in the training set of data. Indeed, generalization errors in these cases are expected to be greater.

Results of V2

In run V2, values of Q_{NaOH} and Q_{HCl} were changed at different moments. Experimental and predicted values of pH are illustrated in Figure 13(a). The values of Q_{NaOH} and Q_{HCl} are shown in Figure 13(b) and (c), respectively. The excellent agreement is confirmed by the dispersion analysis results illustrated in Figure 14.

It could be observed that the pH trend predicted by the model is similar to the experimental one. However, after reduction of the value of Q_{NaOH}, the errors increased. Again, the cause is a lack of data describing similar conditions to the training dataset.

Variance Accounted for (VAF) of the Predicted Values

The performance of prediction model could also be demonstrated by means of the VAF performance index. The VAF index is calculated using:

$$VAF = \left[1 - \frac{var(y - y_m)}{var(y)}\right] \times 100\% \qquad (8)$$

Babuska et al. (1998) commented that the VAF index of models that adequately represent a real system must be greater than 97%. The VAF indices calculated for the prediction model in the experiments are presented in Table VI.

VAF indices calculated for offline validation and for online validation of run V2 were greater than 97%, but in the case of simultaneous disturbances in the acid and basic solution flow rates, the performance was under 97%. However, it must be considered that simultaneous changes in both flow rates are not present in the training dataset because of the different switch times. Besides, this simultaneous disturbance imposes a severe task to the reactor level controller. In Figures 15 and 16, the level of liquid inside the reactor in runs V1 and V2, respectively, is illustrated.

In Figure 15, the oscillations caused by flow rate disturbances are considerably greater than those observed in

Table IV. Consequent parameters of the Takagi–Sugeno prediction model for the reactor outlet effluent pH

pH	q_0	q_1	q_2	q_3	q_4	q_5
1	-2.934×10^{-02}	1.042×10^{-03}	1.432×10^{-03}	-3.555×10^{-03}	-6.181×10^{-03}	9.126×10^{-01}
2	1.626×10^{-02}	4.440×10^{-04}	2.813×10^{-03}	2.313×10^{-04}	-2.107×10^{-03}	8.968×10^{-01}
3	-6.953×10^{-02}	2.654×10^{-03}	1.431×10^{-04}	-3.490×10^{-04}	-4.547×10^{-03}	9.218×10^{-01}
4	4.184×10^{-02}	-1.719×10^{-03}	4.342×10^{-03}	-1.561×10^{-03}	-1.388×10^{-03}	9.079×10^{-01}
5	-5.750×10^{-02}	-1.318×10^{-02}	1.663×10^{-02}	5.447×10^{-05}	-1.683×10^{-03}	1.078×10^{-00}

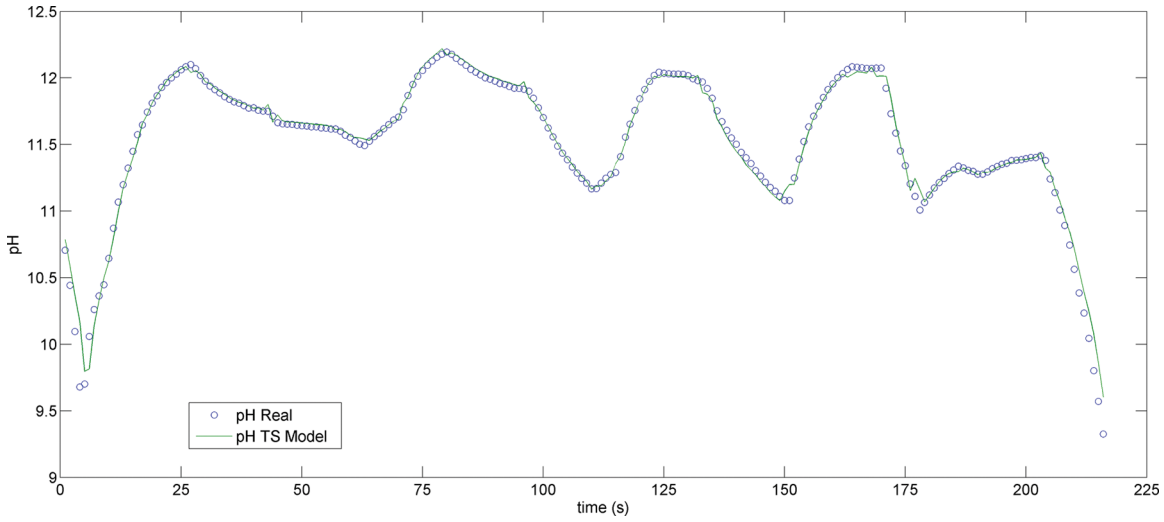

Fig. 9. Validation of prediction model.

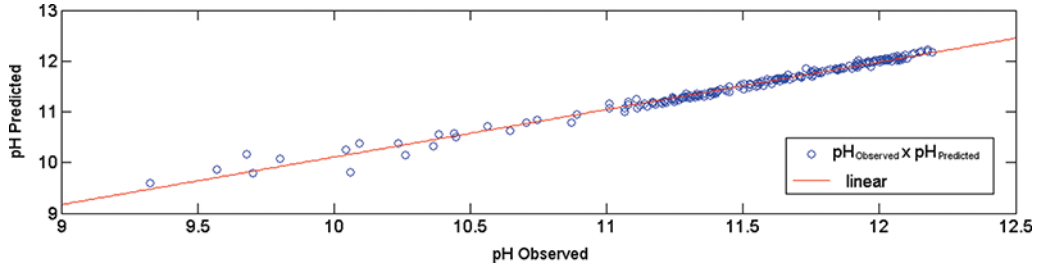

Fig. 10. Dispersion analysis of offline predicted values in comparison with experimental values.

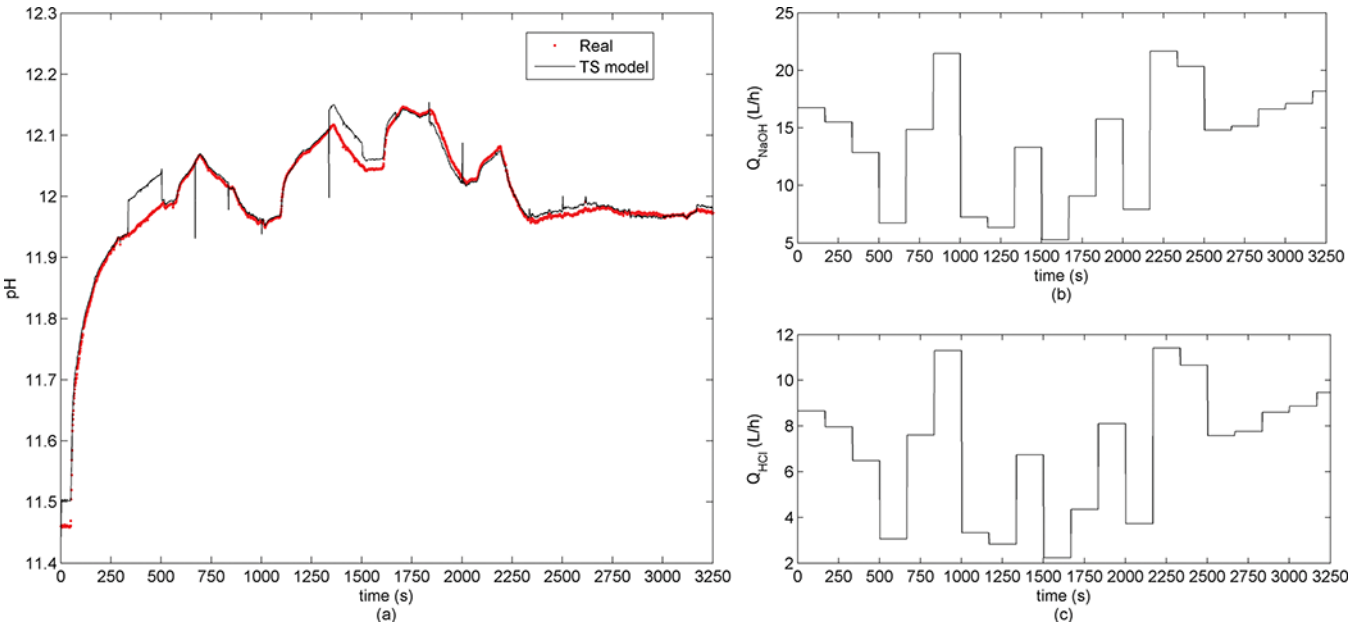

Fig. 11. Online validation of prediction model (run V1): comparison of predicted and real values of pH (a) and disturbances applied to QNaOH (b) and QHCl (c).

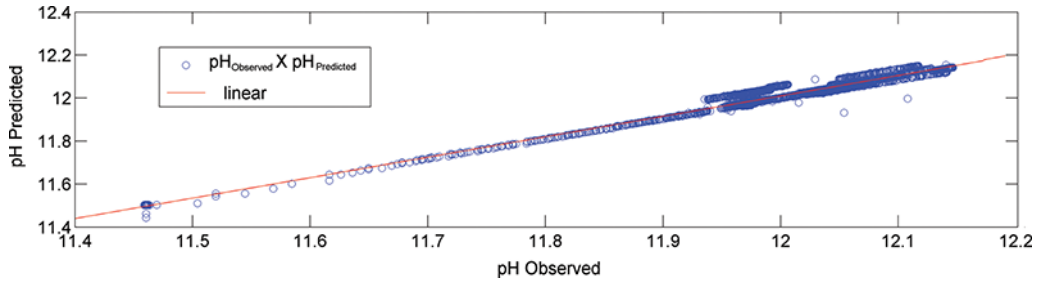

Fig. 12. Dispersion analysis of experimental and online predicted values (run V1).

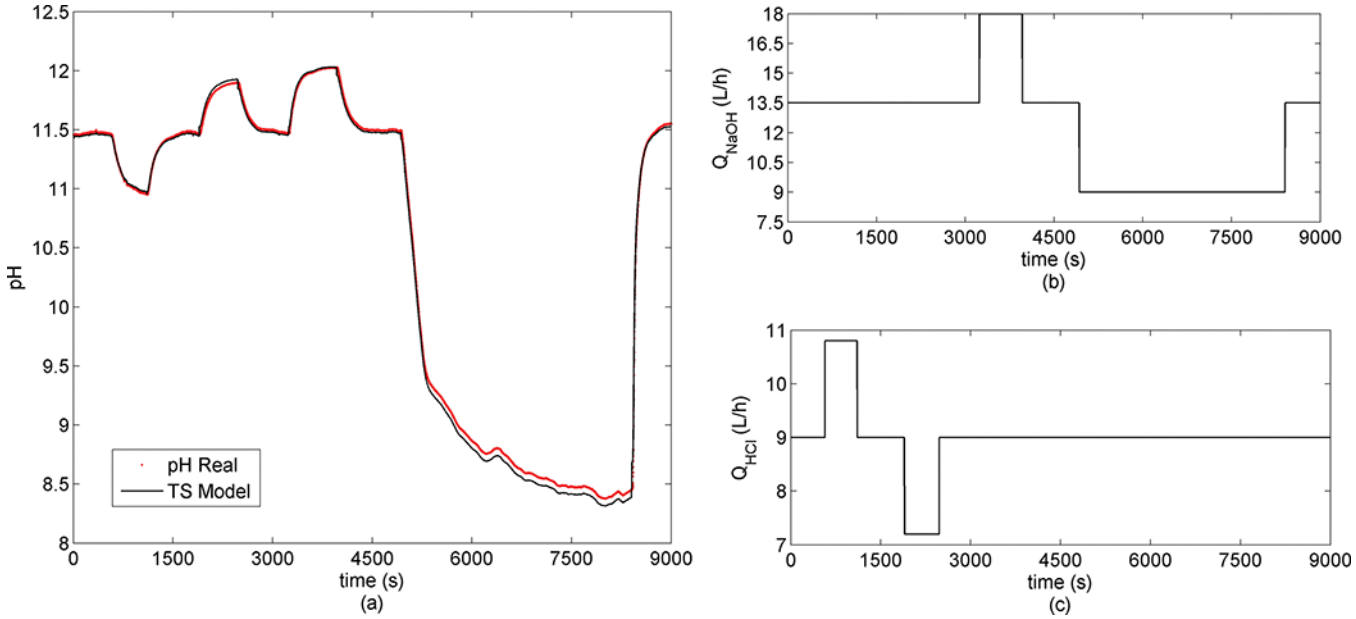

Fig. 13. Online validation of prediction model (run V2): comparison of predicted and real values of pH (a) and disturbances applied to QNaOH (b) and QHCl (c).

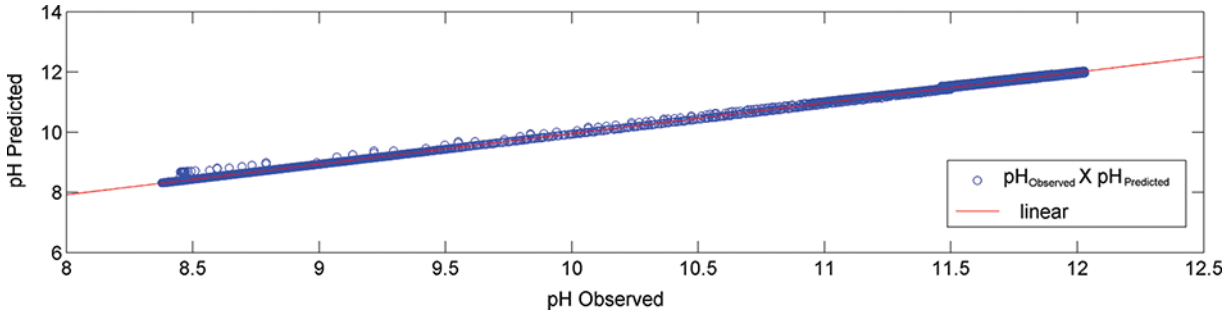

Fig. 14. Dispersion analysis of experimental and online predicted values (run V2).

Table VI. Performance indices for the prediction model in off-line and online validations

Run	VAF (%)	R^2	RMSE
Offline validation	98.55	0.9856	0.0602
Online validation (V1)	96.01	0.9601	0.0189
Online validation (V2)	99.47	0.9997	0.0258

Figure 16. This oscillation contributes to deterioration of the prediction model results, but supports its robustness.

Conclusions

The prediction model attained by using ANFIS architecture was demonstrated to be able to predict the one step-ahead reactor outlet effluent pH precisely. Its efficiency was

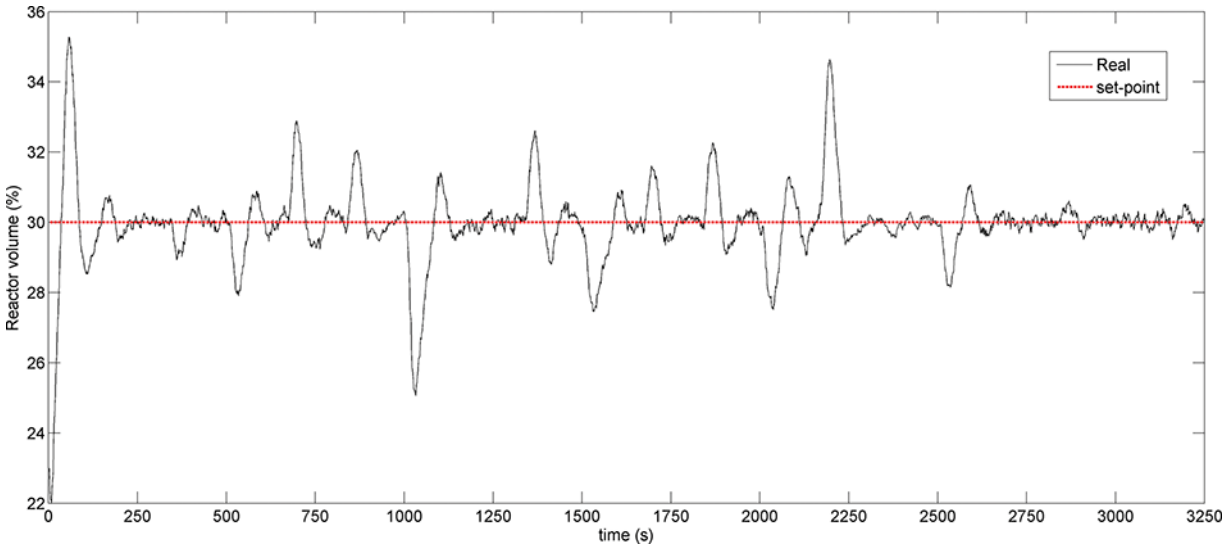

Fig. 15. Level of liquid inside the reactor during run V1.

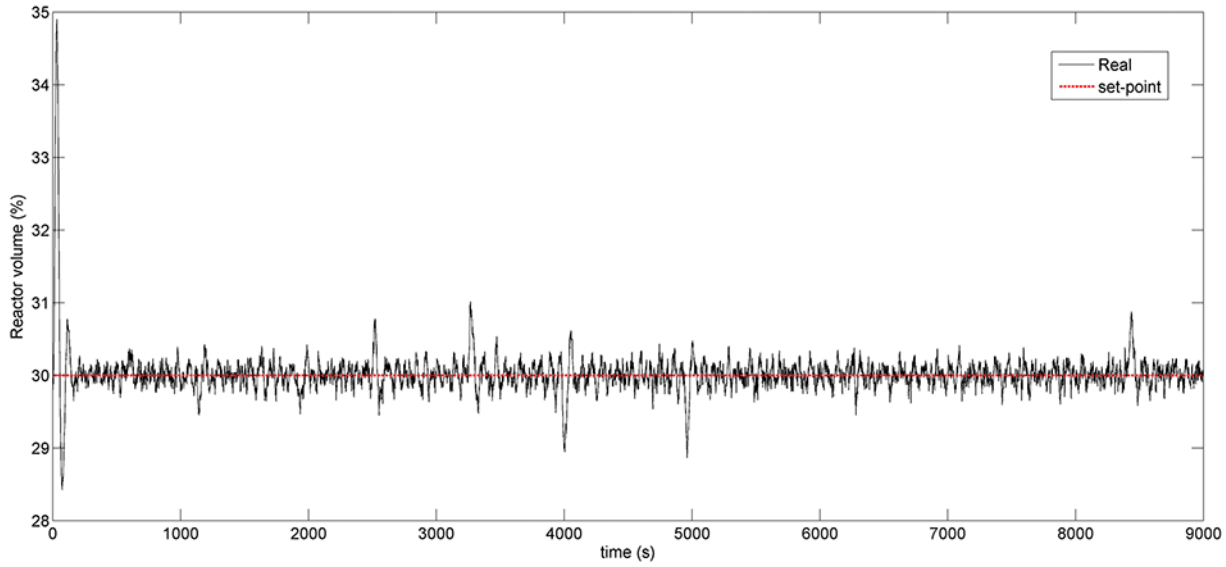

Fig. 16. Level of liquid inside the reactor during run V2.

analyzed in offline and online tests. In tests in which the disturbances were applied in different instants, the VAF values were greater than 97% and the R^2 values were greater than 0.999. Slightly poor performance was attained when the disturbances were applied simultaneously, R^2 equals to 0.960, but as this condition is not present in the training dataset, it could demonstrate the robustness of the approach. Besides, it was demonstrated that ANFIS can provide good performance models directly from process data, without the interference of a human expert.

Funding

The authors are grateful to University Center of FEI for the financial support.

References

Abonyi, J., Nagy, L., and Szeifert, F. (1999). Adaptive fuzzy inference system and its application in modelling and model based control, *Chem. Eng. Res. Des.*, **77**(4), 281–290.

Babuska, R., Roubos, J. A., and Verbruggen, H. B. (1998). Identification of MIMO systems by input-output TS fuzzy models. *The 1998 IEEE international conference on fuzzy systems proceedings*, 4–9 May 1998, Anchorage, AK.

Bath, N. E., and Mcavoy, T. (1990). Use of neural nets for dynamic modeling and control of chemical process systems, *Comput. Chem. Eng.*, **14**(4), 573–583.

Chang, F.-J., and Chang, Y.-T. (2006). Adaptive neuro-fuzzy inference system for prediction of water level in reservoir, *Adv. Water Resour.*, **29**, 1–10.

Chiu, S. L. (1994). Fuzzy model identification based on cluster estimation, *J. Intell. Fuzzy Syst.*, **2**, 267–278.

Draeger, A., Engell, S., and Ranke, H. (1995). Model predictive control using neural networks, *IEEE Control Syst.*, **15**(5), 61–66.

Fernandez De Canete, J., Garcia-Cerezo, A., Garcia-Moral, I., Del Saz, P., and Ochoa, E. (2013). Object-oriented approach applied to ANFIS modeling and control of a distillation column, *Expert Syst. Appl.*, **40**(14), 5648–5660.

Franco, I. C., Dall'agnol, M., Costa, T. V., Fileti, A. M. F., and Silva, F. V. (2011). A neuro-fuzzy identification of non-linear transient systems: application to a pilot refrigeration plant, *Int. J. Refrig.*, **34**, 2063–2075.

Gustafsson, T. K., Skrifvars, B. O., Sandström, K. V., and Waller, V. (1995). Modeling of pH for control, *Ind. Eng. Chem. Res.*, **34**(3), 820–827.

Henson, M. A., and Seborg, D. E. (1994). Adaptative nonlinear control of a pH neutralization process, *IEEE Trans. Control Syst. Technol.*, **2**(3), 169–182.

Jang, J. S. R. (1993). ANFIS: adaptive network based fuzzy inference system, *IEEE Trans. Syst., Man, Cybern.*, **23**(3), 665–685.

Jahedsaravani, A., Marhaban, M. H., and Massinaei, M. (2014). Application of statistical and intelligent techniques for modeling of metallurgical performance of a batch flotation process, *Chem. Eng. Commun.* doi:10.1080/00986445.2014.973944.

Kumbasar, T., Eksin, I., Guzelkaya, M., and Yesil, E. (2011). Adaptive fuzzy model based inverse controller design using BB-BC optimization algorithm, *Expert Syst. Appl.*, **38**(10), 12356–12364.

Mwembeshi, M. M., Kent, C. A., and Salhi, S. (2004). Flexible on-line modeling and control of pH in waste neutralization reactors, *Chem. Eng. Technol.*, **27**(2), 130–138.

Nie, J., Loh, A. P., and Hang, C. C. (1996). Modeling pH neutralization processes using fuzzy-neural approaches, *Fuzzy Sets Syst.*, **78**(1), 5–22.

Paiva, R. P., and Dourado, A. (2004). Interpretability and learning in neuro-fuzzy systems, *Fuzzy Sets Syst.*, **147**, 17–38.

Palancar, M. C., Aragón, J. M., and Torrecilla, J. S. (1998). pH-control system based on artificial neural networks, *Ind. Eng. Chem. Res.*, **37**(7), 2729–2740.

Postlethwaite, B., and Edgar, C. (2000). A MIMO fuzzy model-based controller, *Chem. Eng. Res. Des.*, **78**(4), 557–564.

Seborg, D. E., Mellichamp, D. A., Edgard, T. T., and Doyle Iii, F. J. (2004). *Chemical Process Control*, Wiley, New York, NY.

Valarmathi, K., Devaraj, D., and Radhakrishnan, T. (2009). Intelligent techniques for system identification and controller tuning in pH process, *Braz. J. Chem. Eng.*, **26**, 99–111.

Zhang, J., and Morris, A. J. (1999). Recurrent neuro-fuzzy networks for nonlinear process modeling, *IEEE Trans. Neural Networks*, **10**(2), 313–326.